南京航空航天大学

论 文 集

（二〇〇八年） 第4册

航空宇航学院

《第4分册》

南京航空航天大学科技部编

二〇〇九年五月

航空宇航学院

第四分册

航空宇航学院2008年学术论文清单（0132）

序号	姓名	职称	单位	论文题目	刊物、会议名称	年、卷、期
1	高存法 米耀荣 王保林	教授 教授 教授	0132 外单位 外单位	Eeffects of magneric fields oncracks in a soft ferromagnetic material	engineer fracture mechanics	2008.75.17
2	蒋泉 高存法	博士后 教授	0132 0132	general solution ofstress fields in an electrostrictive material with point charge	第三届全国压电和声波理论及器件技术研讨会论文集	
3	王敏中 Xu Bu 高存法	教授 教授	外单位 外单位 0132	recent general solutions in linear elasticity and their applications	APPLIED MECHANICS REVIEWS	2008.61.03
4	王永健 高存法	博士 教授	0132 0132	the mode III cracks originating from the edge of a circular hole in a piezoelectric solid	international Journal of solids and structures	2008.45.16
5	王永健 高存法	博士 教授	0132 0132	压电体内孔边裂纹的应力强度因子	力学季刊	2008.29.02
6	杨宾华 高存法	博士 教授	0132 0132	interactions between n circular cylindrical inclusions in a piezoelectric matrix	ACTA MECHANICA	2008.197.1-2
7	陈文涛 高存法 杨权权	硕士 教授 硕士	0132 0132 0132	含圆孔功能梯度板在对称载荷作用下的应力分析	第三届全国压电和声波理论及器件技术研讨会论文集	
8	罗家成 高存法	硕士 教授	0132 0132	孔洞放电热应力	力学季刊	2008.29.02
9	张宁 高存法	硕士 教授	0132 0132	椭圆孔周的电致伸缩应力	第三届全国压电和声波理论及器件技术研讨会论文集	
10	古兴瑾 许希武 黄晶	博士 教授 博士	0132 0132 0132	层合复合材料薄板高速冲击损伤研究	南京航空航天大学学报	2008.40.03
11	林智育 许希武	博士 教授	0132 0132	复合材料层板低速冲击后剩余压缩强度	复合材料学报	2008.25.01
12	林智育 许希武	博士 教授	0132 0132	含多椭圆孔（核）复合材料加筋层板的应力集中研究	计算力学学报	2008.25.03
13	徐焜 许希武	博士 教授	0132 0132	Finite element analysis of mechanical properties of 3D five-directional braided composites	Materials Science and Engineering A	2008.487.1-2
14	徐焜 许希武	博士 教授	0132 0132	三维五向编织复合材料宏细观力学性能分析	宇航学报	2008.29.03
15	徐焜 许希武	博士 教授	0132 0132	三维五向矩形编织复合材料的细观结构模型	南京航空航天大学学报	2008.40.02
16	张楠 许希武 潘庆军	博士 教授 副教授	0132 0132 0132	空空导弹威胁下某型飞机的战伤计算与仿真	南京航空航天大学学报	2008.40.02
17	陈伟 许希武	硕士 教授	0132 0132	复合材料双曲率壳屈曲和后屈曲的非线性有限元研究	复合材料学报	2008.25.02
18	喻梅 许希武	硕士 教授	0132 0132	复合材料挖补修理结构的压缩强度分析	中国矿业大学学报	2008.37.05
19	黄再兴	教授	0132	Breaking of global gauge symmetries on a spatial-temporal subdomain	International Journal of Theoretical Physics	2008.47.11
20	黄再兴	教授	0132	Coaxial Stability of Nano-bearings Constructed by the Double-walled Carbon Nano-tube	Nanotechnology	2008.19.04
21	姚寅 黄再兴	博士生 教授	0132 0132	弹性损伤中应变局部化现象的非局部力学模型及其数值模拟	机械强度	2008.30.05
22	姚寅 黄再兴	博士生 教授	0132 0132	非局部核与应变局部化问题解的相关性	南京航空航天大学学报	2008.40.06
23	史治宇 沈林	教授	0132 0132	基于小波方法的时变动力系统参数识别	振动、测试和诊断	2008.28.02

24	S. S. Law S. Q. Wu 史治宇	 教授	外单位 外单位 0132	Moving load and prestress identification using wavelet-based method	Journal of Applied Mechanics	2008. 75. 02
25	李会娜 史治宇	硕士 教授		基于随机激励响应的时变系统物理参数子空间识别方法研究	工程力学	2008. 25. 09
26	许鑫 史治宇	硕士 教授	0132 0132	两种基于随机子空间的模态参数识别方法研究	2008年中国计算力学大会暨第七届南方计算力学学术交流会	
27	杨建国 史治宇	硕士 教授	0132 0132	基于变密度的拓扑优化方法研究及在Patran平台上的二次开发	2008年中国计算力学大会暨第七届南方计算力学学术交流会	
28	朱华兴 史治宇	硕士 教授	0132 0132	基于环境激励响应的两种模态参数识别方法比较	2008年中国计算力学大会暨第七届南方计算力学学术交流会	
29	周储伟 田俊	教授 硕士	0132 0132	Micro-, meso-scale viscoelastic analysis of 3D Woven Composites	第二届国际非均质材料力学会议论文集	
30	田俊 周储伟	硕士 教授	0132 0132	纺织复合材料细观裂纹扩展的局部子划分粘聚力模型	结构强度研究	
31	王鑫伟 甘立飞 张一彗	教授 博士 学士	0132 0132 0132	Differential quadrature analysis of the buckling of thin rectangular plates with cosine-distributed compressive loads on two opposite sides	Advances in Engineering Software	2008. 39. 06
32	戴隆超 王鑫伟	博士 教授	0132 0132	An elliptic thermopiezoelectric inclusion problem in an anisotropic thermopiezoelectric medium	Journal of Intelligent Material Systems and Structures	2008. 19. 03
33	戴隆超 王鑫伟	博士 教授	0132 0132	Analysis of stress field near crack tip based on the electric saturation model	Transactions of NUAA	2008. 25. 03
34	甘立飞 王鑫伟 刘 峰	博士 教授 博士	0132 0132 0132	微分求积单元法分析变曲率井内受径向约束管柱的非线性屈曲	南京航空航天大学学报	2008. 40. 06
35	甘立飞 王鑫伟 王爱军	博士 教授 硕士	0132 0132 0132	矩形薄板受面内非均匀分布载荷稳定性分析	宇航学报	2008. 29. 04
36	刘强 王鑫伟 陈仁文	博士 教授 教授	013 0132 0134	采用正交基函数构造的自适应滤波器	应用科学学报	2008. 26. 05
37	刘剑 王鑫伟	硕士 教授	0132 0132	An assessment of the differential quadrature time integration scheme for non-linear dynamic equations	Journal of Sound and Vibration	2008. 314
38	刘剑 王鑫伟	硕士 教授	0132 0132	基于微分求积法的逐步积分法与常用时间积分法的比较	力学季刊	2008. 39. 02
39	唐玉花 王鑫伟	硕士 教授	0132 0132	关于“平面弹性悬臂梁剪切挠度”的进一步研究	力学与实践	2008. 30. 04
40	王爱军 王鑫伟 陆浦	硕士 教授 硕士	0132 0132 0132	圆柱壳板非线性屈曲的分叉解	南京航空航天大学学报	2008. 40. 05
41	杨珺 王鑫伟	硕士 教授	0132 0132	矩形平面应力扩展有限元及其程序实施	力学季刊	2008. 39. 02
42	张斌 梁拥成 孙慧玉	副教授 讲师 教授	0132 ? 0132	Structural phase transition and failure of nanographite sheets under high pressure: a molecular dynamics study.	Journal of Physics: Condensed Matter	2007. 19. 34
43	周丽 吴新亚 尹强 汪新明	教授 硕士 博士 硕士	0132 0132 0132 0132	基于自适应卡尔曼滤波方法的结构损伤识别实验研究	振动工程学报	2008. 21. 02: 197-202

44	周丽 吴新亚 Yang J. N.	教授 硕士 教授	0132 0132 0132	Experimental study of an adaptive extended kalman filter for structural damage identification	Journal of Infrastructure Systems	2008.14.01: 42-51
45	汪新明 周丽	硕士 教授	0132 0132	基于振动响应的隔震支座的非线性建模及参数估计	振动与冲击	2008.27.01
46	严刚 周丽	博士 教授	0132 0132	基于频率-波数域偏移方法的板结构损伤实时识别	振动工程学报	2008.21.06
47	严刚 周丽	博士 教授	0132 0132	加筋复合材料结构的冲击载荷识别	航空学报	2008.29.05
48	袁晚春 周丽 Yuan F-G	硕士 教授 教授	0132 0132 0132	Wave reflection and transmission in composite beams containing semi-infinite delamination	Journal of Sound and Vibration	2008.313.3-5
49	李成友 周光明 黄再兴 田卫国	硕士生 教授 教授 高工	0132 0132 0132 外单位	34米复合材料风力发电机组叶片屈曲有限元分析	风机技术	2008.207.05
50	蒋凌海 王永亮 王鑫伟	硕士 教授 教授	0132 0132 0132	Buckling analysis of stiffened circular cylindrical panels using differential quadrature element method	Thin-walled Structures	2008.46.04
51	孙慧玉 张斌	教授 副教授	0132 0132	三维编织复合材料力学性能的杂交应力元法	南京航空航天大学学报	2008.40.01
52	刘佳 周光明 王新峰 周储伟	学生 教授	0132 0132	三维机织管状复合材料力学模型与实验验证	China SAMPE 2008国际学术研讨会论文集	
53	边宝龙 黄佩珍 李志刚 高存法	硕士 教授 硕士 教授	0133 0133 0133 0132	内压和外载作用下微裂纹的演化	2008年中国计算力学大会暨第七届南方计算力学学术会议	2008
54	王远鹏 黄佩珍	硕士 教授	0133 0133	裂面形貌扰动对晶内微裂纹演变影响的有限元分析	中南大学学报（自然科学版）	2008.39.04
55	马竞 黄再兴	硕士 教授	0132 0132	具有拉压双模量材料简支梁和悬臂梁稳定性分析	江苏航空	2008.增刊
56	钱元 周光明 刘海	硕士 教授	0132 0132 0132	正交三向复合材料力学性能分析和实验研究	江苏航空	2008.增刊

航空宇航学院2008年学术论文清单（0135）

序号	姓名	职称	单位	论文题目	刊物、会议名称	年、卷、期
2	赵淳生 朱华	教授 讲师	0135 0135	超声电机技术的发展和应用	机械制造与自动化	2008.37.03
3	陈超 赵淳生	副教授 教授	0135 0135	A novel model of ultrasonic motors with effects of radial friction in contact mechanism	Journal of Electroceramics	2008.20.3-4
4	陈超 赵淳生	副教授 教授	0135 0135	柔性转子对行波超声电动机性能的影响	机械工程学报	2008.44.03
5	姚志远 杨东 吴辛 赵淳生	副教授 硕士 博士 教授	0135 0135 0135 0135	Structure Design Method of Bar-structure Linear Ultrasonic Motors	2008IEEE International Ultrasonics Symposium	
6	姚志远 赵淳生 曾劲松 周培	副教授 教授 博士 硕士	0135 0135 0135 0135	Analytical solution on the non-linear vibration of a traveling wave ultrasonic motor	J Electroceram	2008.2
7	周培 姚志远 周凤拯	硕士 副教授	0135 0135	超声电机温升、结构参数和输出特性的相互关系	压电与声光	2008.30.04
8	李华峰 马春苗 冒俊	教授 硕士 硕士	0135 0135 0135	维持超声电机工作状态恒定的驱动控制器	中国电机工程学报	2008.28.36
9	彭瀚? 杨淋 李华峰 赵淳生	博士 博士 教授 教授	0135 0135 0135 0135	离子聚合物——金属复合物发展综述	微特电机	2008.36.02
10	孙宏超 李华峰	硕士 教授	0135 0135	Intelligent Video Surveillance System Based on Ultraasonic Motors	SMSAE/SMEBA2008国际研讨会	
11	王红占 李华峰	硕士 教授	0135 0135	A psoc-based parallel inductor connection driver of ultrasonic motor	ICEMS2008	
12	张建辉 黎毅力 刘菊银 徐宇哲	教授	0135 外单位 外单位 外单位	“Y”形流管无阀压压电泵流场分析	北京工业大学学报	2008.34.02
13	张建辉 路计庄 夏齐霄 寇杰 任刚	教授	0135 外单位 外单位 外单位	细胞或高分子输送用“Y”形流管无罚压电泵的工作原理及流量特性	机械工程学报	2008.44.09
14	叶芳 黎毅力 张建辉	硕士 教授	0135 0135	Dynamic research on actuator for vvalveless piezoelectric pump with Y-shape tube “Y”形流管无阀压电泵驱动器的动态研究	光学精密工程	2008.16.12
15	丁庆军 姚志远 郑伟 赵淳生	副教授 副教授 博士后 教授	0135 0135 0135 0135	行波型超声电机定子摩擦材料的研制及其摩擦磨损性能研究	摩擦学学报	2007.27.06
16	金家楣 赵淳生	讲师 教授	0135 0135	A novel Traveling Wave Ultrasonic Motor Using a Bar Shaped Transducer	JOURNAL OF UNIVERSITY OF TECHNOLOGY-MATERIALS SCIENCE EDITION	2008.23.06
17	金家楣 赵淳生	讲师 教授	0135 0135	Characteristic matching between stator and rotor in standing-wave - type ultrasonic motors	Journal of Electroceramics	2008.20.3-4
18	金家楣 张建辉 赵淳生	讲师 教授 教授	0135 0135 0135	Elliptic motions on modal conversion ultrasonic motors/模态转换型超声电机中的椭圆运动	南京航空航天大学学报（英文版）	2008.25.04

19	金家楣 赵淳生	讲师 教授	0135 0135	Liner stepping ultrasonic motor	Journal of Electroceramics	2008.20.3-4
20	金家楣 张建辉 赵淳生	讲师 教授 教授	0135 0135 0135	单振子激励的面内行波旋转超声电机原理	湖南大学学报（自然科学版）	2008.35.12
21	金家楣 张建辉 赵淳生	讲师 教授 教授	0135 0135 0135	环形定子面内回转旋转超声电机原理	南京航空航天大学学报	2008.40.06
22	金家楣 张建辉 赵淳生	讲师 教授 教授	0135 0135 0135	新型多轴旋转超声电机原理	振动、测试与诊断	2008.28.04
23	金家楣 时运来 李玉宝 赵淳生	讲师 博士生 博士生 教授	0135 0135 0135 0135	新型惯性式直线超声电压电电机的运动机理及实验研究 Research on novel inertial linear ultrasonic piezoelectric motor	光学精密工程	2008.16.12
24	朱华 陈超 赵淳生	讲师 副教授 教授	0135 0135 0135	行波型杆式超声电机的动力学分析与性能仿真	振动与冲击	2008.27.06
25	朱华 罗来慧 陈超 赵淳生	讲师 讲师 副教授 教授	0135 0135 0135 0135	Modeling of A Cylindrical Ultrasonic Motor Based on the Single Crysta	Journal of Electroceramics	2008.20.3—4
26	朱华 曾劲松 赵淳生	讲师 博士生 教授	0135 0135 0135	杆式超声电机定子的动力学分析与优化设计	中国机械工程	2008.19.21

Engineering Fracture Mechanics 75 (2008) 4920–4924

Contents lists available at ScienceDirect

Engineering Fracture Mechanics

journal homepage: www.elsevier.com/locate/engfracmech

Influence of mechanical stresses on partial discharge in a piezoelectric solid containing cavities

Cun-Fa Gao *

College of Aerospace Engineering, Nanjing University of Aeronautics and Astronautics, Nanjing 210016, China

ARTICLE INFO

Article history:
Available online 3 July 2008

Keywords:
Piezoelectric ceramics
Crack
Partial discharge
Mechanical stress

ABSTRACT

For a piezoelectric solid with an air-filled elliptic cavity, the two-dimensional problems of partial discharge inside the cavity are studied when the solid is subjected to combined mechanical stress and electric field. Based on the law of Paschen, the influence of mechanical stress on partial discharge is discussed. It is shown from the obtained results that the applied mechanical stress can retard or enhance the occurrence of partial discharge, which is dependent on the signs of applied electric fields. It is also found that for a mathematical crack (with zero initial width), partial discharge may not happen even when the significantly high mechanical and electric loadings are applied within the range of practical interest.

1. Introduction

When a dielectric solid containing an air-filled thin cavity is electrically loaded, the electric field inside the cavity may be greatly enhanced in magnitude than the applied electric loading for the dielectric solids having higher dielectric constant than air. When the induced electric field reaches a critical value, partial discharge (PD) of air may occur inside the cavity [1]. In high-voltage insulation systems, the occurrence of PD is highly undesirable because PD makes the insulating materials degrade rapidly both physically and chemically, and finally results in the breakdown of the dielectric and limits the lifetime of an insulation system [2]. For this reason, a lengthy literature has been developed on the subject of PD. An excellent review of the subject can be found in the work of Druyvesteyn and Penning [3] who summarized the important theoretical and experimental contributions made before 1940. In recent decades, great progress was made on understanding cavity discharges [4–10]. However, the pioneering works were mainly for the cases of PD in an isotropic dielectric solid under pure electric loading. With increasingly wide applications of piezoelectric materials in smart materials structures, it is also essential to explore the PD of defects in piezoelectric solids. Electric filed strength inside defects is one of important factors causing PD [1]. Different from the cases of dielectric solids, the mechanical stress can produce the high electric field inside thin defects [11,12], and thus this work is focused on the study of the influence of mechanical stress on PD in a piezoelectric solid.

2. Description of the problem

Consider a transversely isotropic piezoelectric solid refereed to a Cartesian coordinate system $x_1 - x_2 - x_3$. The solid is polarized along the positive x_2 direction, and it is reduced by a long cylinder cavity. The cavity is oriented along the x_3 axis and whose cross section is an ellipse. We investigate a two-dimensional (2D) problem taking placing in the $x_1 - x_2$ plane that

* Tel.: +86 25 8489 6237; fax: +86 25 8489 1422.
E-mail address: cfgao@nuaa.edu.cn

0013-7944/$ - see front matter © 2008 Elsevier Ltd. All rights reserved.
doi:10.1016/j.engfracmech.2008.06.022

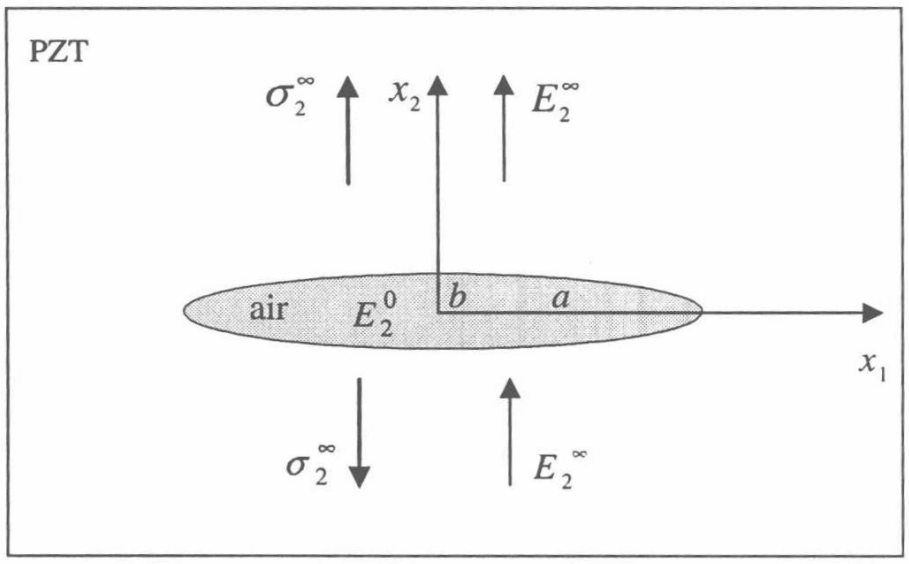

Fig. 1. Elliptic cavity in a piezoelectric solid under combined mechanical stress and electric field.

is subjected to uniform mechanical stress σ_2^∞ and electric field E_2^∞, as shown in Fig. 1. Additionally, assume that the cavity is filled with air.

In general, the constitutive equations of piezoelectric solids can be expressed as

$$\sigma = \mathbf{c}\gamma - \mathbf{e}\mathbf{E}, \quad \mathbf{D} = \mathbf{e}^T\gamma + \varepsilon\mathbf{E} \tag{1}$$

where $\boldsymbol{\sigma}$, $\boldsymbol{\gamma}$, $\mathbf{E}$ and $\mathbf{D}$ are stress, strain, electric fields and electric displacement vectors, respectively. $\mathbf{c}$, $\mathbf{e}$ and ε stands for the elastic, piezoelectric and dielectric constants, respectively.

For the present 2D problem, all field variables both in the solid and inside the cavity are functions of x_1 and x_2 only. The components of stress fields and electric displacements can be obtained from

$$[\sigma_{11}, \sigma_{12}, \sigma_{13}, D_1]^T = -\phi_{,2}, [\sigma_{12}, \sigma_{22}, \sigma_{23}, D_2]^T = \phi_{,1} \tag{2}$$

where $\mathbf{u}$ and ϕ are the generalized displacement function and stress function, respectively. The general solution for $\mathbf{u}$ and ϕ are [13]

$$\mathbf{u} = \mathbf{A}\mathbf{f}(z) + \overline{\mathbf{A}\mathbf{f}(z)}, \quad \phi = \mathbf{B}\mathbf{f}(Z) + \overline{\mathbf{B}\mathbf{f}(Z)} \tag{3}$$

where $\mathbf{A}$ and $\mathbf{B}$ are two constant matrices, and $\mathbf{f}(z)$ is an unknown complex vector.

After $\mathbf{f}(z)$ is determined from the given boundary conditions, all field variables can be obtained. In the present work, we do not deal with the detail about the solution of $\mathbf{f}(z)$, and only give the result of the electric field inside the cavity to discuss PD inside it.

3. Electric field inside the cavity

For an elliptic cavity with arbitrary semi-axis a and b, the component of electric displacement D_2^0 inside it can be expressed as [12]

$$D_2^\infty - D_2^0 = \frac{b(D_2^\infty - \varepsilon_0 E_2^\infty) + \varepsilon_0 H_{42}\sigma_2^\infty a/2}{b + a\varepsilon_0/\varepsilon_{\text{eff}}} \tag{4}$$

where D_2^∞ is the electric displacement at infinity, ε_0 is the dielectric constant of air, $\varepsilon_{\text{eff}} = -2/H_{44} > 0$, and H_{42} and H_{44} are the components of the matrix $\mathbf{H}$ defined as $\mathbf{H} = 2\text{Re}[i\mathbf{A}\mathbf{B}^{-1}]$.

According to constitutive Eq. (1), D_2^∞ can be expressed through the electric field and strain at infinity. For the present problem, it can be shown that D_2^∞ has the form

$$D_2^\infty = \varepsilon_2^{\text{M}} E_2^\infty \tag{5}$$

where

$$\varepsilon_2^M = \left(\frac{e_{15}^2}{c_{44}} + \varepsilon_{11}\right) \tag{6}$$

Using Eqs. (4) and (5), the resulting electric field inside the cavity is

$$E_2^0 = \frac{D_2^0}{\varepsilon_0} = \frac{\left(\frac{b}{a} + \frac{\varepsilon_2^{\text{M}}}{\varepsilon_{\text{eff}}}\right)E_2^\infty - \frac{H_{42}}{2}\sigma_2^\infty}{\frac{b}{a} + \frac{\varepsilon_0}{\varepsilon_{\text{eff}}}} \tag{7}$$

For an isotropic dielectric solid, one has $\varepsilon_2^M = \varepsilon_{\text{eff}} = \varepsilon_{\text{M}}$, and Eq. (7) becomes, under pure electric field, into [14]

$$E_2^0 = \frac{\frac{b}{a}+1}{\frac{b}{a}+\frac{\varepsilon_0}{\varepsilon_{\text{M}}}} E_2^\infty$$

where ε_{M} is the dielectric constant of the solid.

Since $H_{42} > 0$ in general cases, Eq. (7) shows that for a positive electric field E_2^∞ (in the positive x_2 direction), the mechanical stress σ_2^∞ always reduces the electric field strength in the cavity. Especially, when the ratio of the applied mechanical stress to the applied electric field satisfies the following condition:

$$\frac{\sigma_2^\infty}{E_2^\infty} = \frac{2}{H_{42}}\left(\frac{b}{a}+\frac{\varepsilon_2^{\text{M}}}{\varepsilon_{\text{eff}}}\right) \tag{8}$$

Eq. (8) results in zero electric field E_2^0. This means that PD may not happen under the specified loading condition.

On the other hand, for an applied negative electric load, the contributions from the mechanical and electric loading to E_2^0 are the same in sign. Thus, the magnitude of E_2^0 inside the cavity becomes

$$E_2^0 = \frac{\left(\frac{b}{a}+\frac{\varepsilon_2^{\text{M}}}{\varepsilon_{\text{eff}}}\right)E_2^\infty + \frac{H_{42}}{2}\sigma_2^\infty}{\frac{b}{a}+\frac{\varepsilon_0}{\varepsilon_{\text{eff}}}} \tag{9}$$

In this case, the mechanical stress enhances the electric field inside the cavity. It is also found from Eqs. (7) and (9) that for the above two cases, E_2^0 may become very high in magnitude as the cavity becomes thin. When E_2^0 is enhanced to a critical value, PD may happen. Below we explore the effect of applied mechanical stress on PD.

4. Townsend discharge

In this work, we only study the Townsend-type discharge. For the Townsend-type discharge, the critical condition for PD in the cavity can be written as,

$$E_2^0 > E_{\text{b}} \tag{10}$$

where E_{b} is the breakdown electric field of PD.

For an elliptic cavity studied in the present work, it is shown from Eq. (4) that the electric field within the cavity is uniform everywhere before partial discharge, when the solid is subjected to the far-field mechanical/electric loading. In this case, the Paschen law [1] is a good approximation to predict whether partial discharge happens or not, for the gas under uniform electric field. Based on the Paschen's law, the breakdown field strength is a unique function of the pressure p and cavity width d, and it can be determined experimentally. We use the result of Crichton et al. [4]:

$$\frac{E_{\text{b}}}{p} = \frac{6.72}{\sqrt{pd}} + 24.36\left(\frac{\text{kV}}{\text{cm bar}}\right) \tag{11}$$

where $d \approx 2b$ for a very thin cavity. It has been shown that for air at standard temperature (20 °C) and pressure ($p = 1$ bar), the breakdown field strength calculated from Eq. (11) agrees well with experimental values.

Taking $p = 1$ bar, Eq. (11) can be rewritten as

$$E_{\text{b}} = \frac{0.672}{\sqrt{d}} + 2.436\left(\frac{\text{MV}}{\text{m}}\right) \tag{12}$$

where d is expressed in cm.

The PZT-5H is selected as a model material. The matrices **A** and **B** in Eq. (3) can be calculated and then the matrix **H** can be determined [15]. The final results are listed as follows:

$$\begin{aligned} &H_{22} = 3.21\times10^{-11}\ \text{m}^2/\text{N},\quad H_{42} = 2.56\times10^{-2}\ \text{m}^2/\text{C},\quad H_{44} = -9.16\times10^{7}\ \text{Vm/C}\\ &\varepsilon_{\text{eff}} = 2.18\times10^{-8},\quad \varepsilon_2^{\text{M}} = 2.3\times10^{-8}\ \text{N/V}^2 \quad \text{and} \quad \varepsilon_0 = 8.85\times10^{-12}\ \text{N/V}^2 \end{aligned} \tag{13}$$

For a cavity with $a = 1$ cm, using the above data, one has from Eq. (7), that

$$E_2^0 = \frac{(d+2.1)E_2^\infty - 25.6\times10^{-3}\sigma_2^\infty}{d+8\times10^{-4}}\left(\frac{\text{V}}{\text{m}}\right) \tag{14}$$

when an applied positive electric field E_2^∞ and a mechanical stress σ_2^∞ are applied.

Substituting Eqs. (12) and (14) into Eq. (10) results in

$$(d+2.1)E_2^\infty - 25.6\times10^{-3}\sigma_2^\infty > \left(d+8\times10^{-4}\right)(0.672/\sqrt{d}+2.436)\times10^6 \tag{15}$$

Similarly, for an applied negative electric field, Eqs. (9)–(11) leads to

$$(d+2.1)E_2^{\infty}+25.6\times10^{-3}\sigma_2^{\infty}>(d+8\times10^{-4})(0.672/\sqrt{d}+2.436)\times10^{6} \tag{16}$$

Eqs. (15) and (16) can be applied to predict if PD may happen. Shown in Fig. 2 is the variation of the magnitude of E_2^0 inside the cavity and the Paschen's curve E_b as a function of the cavity width d. It can be found that the curve No. 1 has a cross point with that of E_b when a positive electric loading of $E_2^{\infty}=0.4$ MV/m is only applied. This indicates that PD may happen under the pure electric field. But, if a mechanical stress of $\sigma_2^{\infty}=30$ MPa is added, the electric field strength E_2^0 (shown as the curve No. 2) is always lower thanE_b, and thus PD may not happen any more. On the other hand, when a negative electric field of $E_2^{\infty}=50\ kV/m$ together with a mechanical stress of $\sigma_2^{\infty}=30$ MPa is applied, Fig. 3 shows that PD may happen, but it does not happen if the mechanical load is removed. In a word, the applied mechanical stress may take the retarding or enhancing effects on the occurrence of PD, which is dependent on the directions of applied electric fields.

When the thin cavity degenerates into a mathematical crack (with zero initial width), the electric field inside the crack approaches a limiting value $E_2^0=\varepsilon_2^M E_2^{\infty}/\varepsilon_0$ from Eq. (7) for the case of pure electric loading. However, it is shown from Eq. (12) that E_b is in proportion to $d^{-1/2}$ and goes to the infinity. This means that for the mathematical crack, it is difficult for PD to happen under pure electric loading. When a uniform mechanical σ_2^{∞} is added, the crack opens to an elliptical cavity with $d=2b_0$, where b_0 stands for the crack opening calculated from [12]

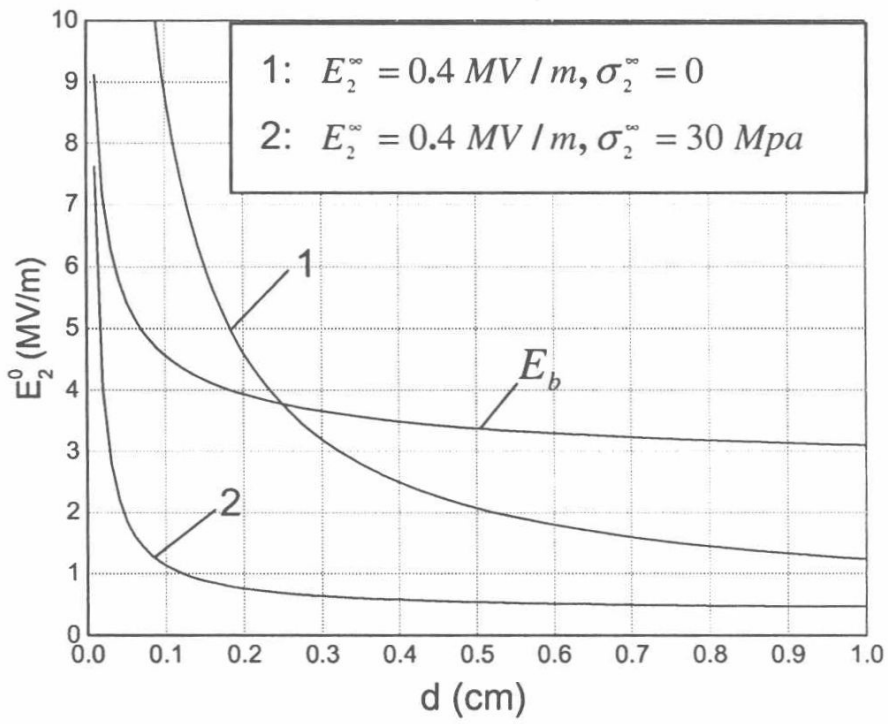

Fig. 2. Effect of mechanical stress together with an applied positive electric field on PD.

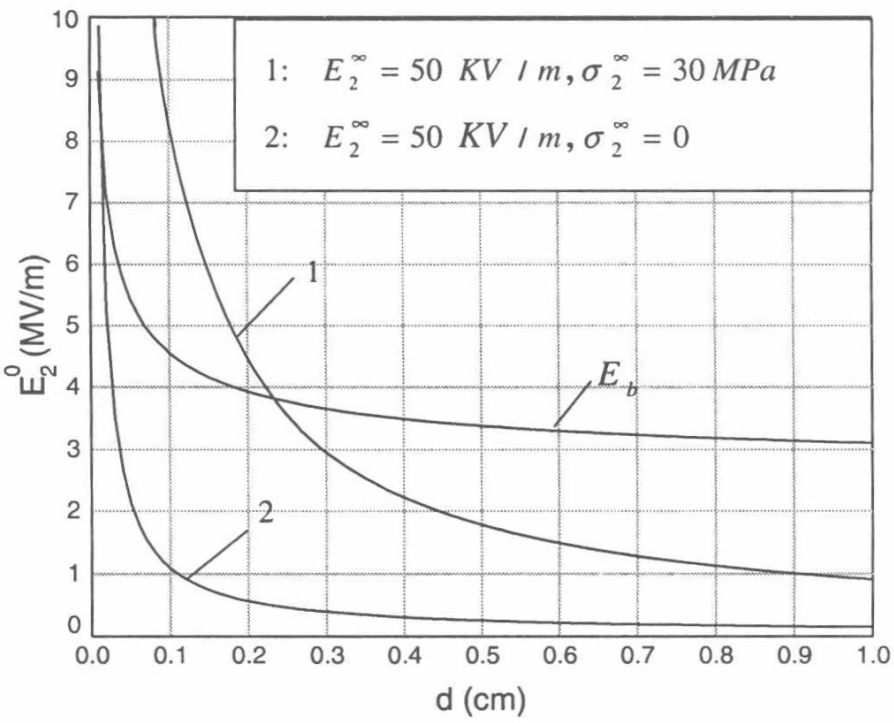

Fig. 3. Effect of mechanical stress together with an applied negative electric field on PD.

$$d = \frac{1}{2}\left(H_{22} - \frac{H_{42}^2}{H_{44}}\right)\sigma_2^{\infty} a \tag{17}$$

As an example, we take $\sigma_2^{\infty} = 100$ MPa and the crack length $a = 1$cm. Using Eq. (15) with Eqs. (13) and (17), we finally obtain the needed positive electric loading for PD as $E_2^{\infty} = 1.3$ MV/m. The loading is beyond the strength limit of the materials. Thus, PD may not happen in a mathematical crack even when the significantly high mechanical and electric loadings are applied within the range of practical interest.

5. Conclusions

We studied the influences of mechanical stress on PD in an air-filled elliptic cavity in a piezoelectric solid. It is found that the mechanical stress may retard or enhance the occurrence of PD, which is dependent on the direction of the applied electric field. However, for a mathematical crack, PD may not happen even if a significantly high mechanical stress is applied. Finally, it should be noted that for a given electric loading, one can control the occurrence of PD in a cavity through applying a proper mechanical stress that satisfies the Eq. (8), because the mechanical stress can change the strength of electric fields inside the cavity.

Acknowledgement

The author would like to acknowledge the support of the National Natural Science Foundation of China (A10672076).

References

[1] Bartnikas R. Corona discharge processes in voids. In: Engineering dielectrics: corona measurement and interpretation, vol. 1. US: Springer; 1979. p. 669.
[2] Kuffel E, Zaengl WS, Kuffel J. High voltage engineering: fundamentals. 2nd ed. Oxford: Butterworth-Heineman; 2000.
[3] Druyvesteyn MJ, Penning FM. The mechanism of electrical discharges in gases of low pressure. Rev Mod Phys 1940;12:87–174.
[4] Crichton GC, Karlsson PW, Pedersen A. Partial discharges in ellipsoidal and spheroidal voids. IEEE Trans Dielectr Electr Insul 1989;24:335–42.
[5] Niemeyer L. A generalized approach to partial discharge modeling. IEEE Trans Dielectr Electr Insul 1995;2:510–28.
[6] Gutfleisch F, Niemeyer L. Measurement and simulation of PD in epoxy voids. IEEE Trans Dielectr Electr Insul 1995;2:729–43.
[7] Salama MMA, Rizk MS, Hackam R. Electrical stress and inception voltage of discharges in gaseous cavities in an anisotropic dielectric material. J Appl Phys 1986;60:2600–8.
[8] McAllister IW, Chrichton GC. Influence of bulk dielectric polarization upon partial discharge transients – effect of heterogeneous dielectric geometry. IEEE Trans Dielectr Electr Insul 2000;7:124–32.
[9] Nikonov V, Bartnukas R, Wertheiner MR. The influence of dielectric surface charge distribution upon the partial discharge behavior in short air gaps. IEEE Trans Plasma Sci 2001;29:866–74.
[10] Anderson RA, Lagasse RR, Russick EM, Schroeder JL. Pulsed electrical breakdown of a void-filled dielectric. J Appl Phys 2002;91:5962–71.
[11] McMeeking RM. Towards a fracture mechanics for brittle piezoelectric and dielectric materials. Int J Fract 2001;108:25–41.
[12] Zhang TY, Gao CF. Fracture behaviors of piezoelectric materials. Theor Appl Fract Mech 2004;41:339–79.
[13] Suo Z, Kuo CM, Barnett DM, Willis JR. Fracture mechanics for piezoelectric ceramics. J Mech Phys Solids 1992;40:739–65.
[14] Gao CF, Noda N. Effects of partial discharges on crack growth in dielectrics. Appl Phys Lett 2005;86. Article no.: 162904.
[15] Landis CM. Energetically consistent boundary conditions for electromechanical fracture. Int J Solids Struct 2004;41:6291–315.

Engineering Fracture Mechanics 75 (2008) 4863–4875

Contents lists available at ScienceDirect

Engineering Fracture Mechanics

journal homepage: www.elsevier.com/locate/engfracmech

Effects of magnetic fields on cracks in a soft ferromagnetic material

Cun-Fa Gao [a,b], Yiu-Wing Mai [b,*], Bao-Lin Wang [b]

[a] College of Aerospace Engineering, Nanjing University of Aeronautics and Astronautics, Nanjing 210016, China
[b] Centre for Advanced Materials Technology (CAMT), School of Aerospace, Mechanical and Mechatronic Engineering J07, University of Sydney, Sydney, NSW 2006, Australia

ARTICLE INFO

Article history:
Available online 1 July 2008

Keywords:
Cracks
Soft ferromagnetic materials
Effect of magnetic fields

ABSTRACT

The 2D problem of a soft ferromagnetic solid with a finite crack under a uniform magnetic field has been studied based on the linear theory of Pao and Yeh. Especially, in this work, the Maxwell stresses induced by the applied magnetic field are taken into account in the boundary conditions not only along the crack surfaces, but also at infinity. Based on these boundary conditions, the related boundary-value problem is solved by using Muskhelishvili's complex variable method to obtain the complex potentials. Thus, it is found that the obtained complex potentials are constant, which indicates that both magnetic fields and stress are uniform in the solid. This implies that if only a pure magnetic field is applied, it has no effects on a crack in a soft ferromagnetic solid. To confirm this result, the same boundary-value problem is solved by the integral transform technique, which shows the same finding as that by using the complex variable method. This outcome is consistent with available experimental data but different to previously published theoretical results.

1. Introduction

Ferromagnetic materials have wide applications in transformers, generators, induction coils, electric motors, etc. Therefore, magnetoelastic coupling problems in ferromagnetic materials have received growing interest in recent years. Pioneering studies on magnetoelastic theory include those of Dunkin and Eringen [1], Tiersten [2] and Brown [3]. Since these early theories are nonlinear and complicated to use, a linearized version of Brown's theory was developed by Pao and Yeh [4] for a soft ferromagnetic solid with a low level of hysteresis loop and a small remanent magnetization. Their contribution has enabled analytical results to be obtained for the boundary-value problems of magnetoelastic interaction. Clearly, different results will be obtained with different boundary conditions. Currently, there are two kinds of commonly used boundary conditions: one considers the Maxwell stress in the boundary conditions along the crack surfaces, and the other does not. Similar to what is done in piezoelectric materials, the first kind of boundary condition may be called a magnetically permeable model, but the second a magnetically impermeable model. With the magnetically permeable model, Shindo [5] was first to study the linear magnetoelastic problem of a soft ferromagnetic elastic solid with a finite crack using Pao and Yeh's theory and the integral transform technique. Further studies were extended to cases of different crack geometry and loading configuration [6–10]. It was found that application of only a magnetic field could produce singular stresses near the crack tips. Further, there is a critical magnetic field b_c which is unrelated to crack length but which results in an infinite value of the stress intensity factor [5], that is, elastic equilibrium is impossible. More recently, Liang et al. [11,12] developed a complex potential method for 2D problems of cracks in a homogeneous and a dissimilar soft ferromagnetic solid, respectively, using the permeable crack model. In contrast, Lin and Yeh [13], and Lin and Lin [14] adopted the impermeable crack model to study

* Corresponding author. Address: School of Aerospace, Mechanical and Mechatronic Engineering, University of Sydney, Sydney, NSW 2006, Australia.
E-mail addresses: cfgao@nuaa.edu.cn (C.-F. Gao), y.mai@usyd.edu.au (Y.-W. Mai), b.wang@usyd.edu.au (B.-L. Wang).

0013-7944/$ - see front matter © 2008 Elsevier Ltd. All rights reserved.
doi:10.1016/j.engfracmech.2008.06.013

crack problems in soft ferromagnetic materials based on a simplified version of the linear theory of Pao and Yeh [4], which neglects all magnetic quantities related to deformation. It was also found that an applied magnetic field could produce singular stresses in the solid with a mathematical crack. In particular, Fil'shtinkskii [15] solved a plane problem in a soft ferromagnetic medium containing some mathematical cuts in the initial state using a complex function method with the impermeable crack model. He arrived at a similar conclusion that pure magnetic fields have effects on crack growth. He also obtained a critical magnetic field b_c at which elastic equilibrium is not possible. In summary, nearly all the available theoretical predictions in the literature show that a magnetic field can produce singular stresses in a soft ferromagnetic solid with mathematical cracks, if they are magnetically permeable or not. Conversely, there are some experimental studies on the effects of magnetic field on fracture toughness of soft ferromagnetic materials, and it was found that no measurable effect occurred even for a magnetic field that exceeded 75 T [16,17], though the sample size was finite. Hence, there is an inconsistency between theoretical results and experimental observations on the magnetic field effect on a mathematical crack in a soft ferromagnetic solid. In fact, when a soft ferromagnetic solid with cracks is exposed to air, the Maxwell stresses will be induced not only on the crack faces, but also on the outside surface of the solid. This means that, not only on the crack faces but also at infinity, the Maxwell stresses must be taken into account in the boundary conditions.

Motivated by this viewpoint, in this paper we re-visit a mode-I mathematical crack in a soft ferromagnetic solid to investigate the effects of applied magnetic fields on cracks. The paper is arranged as follows: in Section 2, basic equations are outlined according to Pao and Yeh's theory [4], where all magnetic quantities are divided into two parts: one corresponds to the rigid body state and the other the perturbation state. Then, the solutions of magnetic fields for the rigid body state are given in Section 3. Presented in Section 4 are the field expressions of elastic stresses and displacements for the perturbation state. Explicit expressions of boundary conditions on the crack faces and at infinity are shown in Section 5. Solutions for complex potentials of a crack under a pure magnetic field are derived, and explicit and closed-form results are obtained in Section 6. In addition, the present crack problem is also solved based on the integral transform technique in Appendix B. Finally, discussions on the effects of magnetic fields on a crack are given in Section 7.

2. Basic equations

Consider an isotropic soft ferromagnetic solid. Pao and Yeh [4] developed a linear theory based on the assumption that all magnetic quantities in a deformable solid can be divided into two parts: (a) those components in the rigid body state; and (b) those components in the perturbation state. Thus, the components of magnetic-induction **B**, magnetization **M**, and magnetic field strength **H** can be represented by

$$B_i = B_i^0 + b_i, \quad H_i = H_i^0 + h_i, \quad M_i = M_i^0 + m_i, \quad (i = 1,2,3), \tag{1}$$

where B_i^0, H_i^0 and $M_i^0 = \chi H_i^0$ denote magnetic quantities in the 'rigid' un-deformed state; b_i, h_i and $m_i = \chi h_i$ are perturbation terms standing for the contributions of elastic deformation to the magnetic quantities, and χ is magnetic susceptibility.

(A) Rigid body state: B_i^0, H_i^0 and M_i^0 can be determined only by solving the magneto-static boundary-value problems with the following equations:

$$e_{ijk}H_{k,j}^0 = 0, \quad B_{i,i}^0 = 0, \tag{2}$$

where e_{ijk} is permutation tensor and a comma means partial differentiation. Also, we have

$$B_i^0 = \mu_0(H_i^0 + M_i^0) = \mu_0(1+\chi)M_i^0 = \mu_0\mu_r H_i^0 = \mu_1 H_i^0, \tag{3}$$

and $\mu_1 = \mu_0\mu_r$, in which μ_0 is the absolute permeability of vacuum, and $\mu_r = (1+\chi)$ is the relative magnetic permeability of the solid.

Along the boundary of an un-deformed body with an outer normal n_i, the boundary conditions are given by

$$e_{ijk}n_j[\![H_{k^0}]\!] = 0, \quad n_k[\![B_k^0]\!] = 0, \tag{4}$$

where $[\![\ ]\!]$ represents the discontinuity jump across the boundary.

(B) Perturbation state: Consider the case in which $|M_j^0 u_{i,j}| << |m_i|$, where u_i is the displacement. The equilibrium equations become

$$e_{ijk}h_{k,j} = 0, \quad b_{i,i} = 0, \quad b_i = \mu_1 h_i, \tag{5}$$

$$\left(t_{ij} + t_{ij}^M\right)_{,i} = 0, \tag{6}$$

where $\left(t_{ij} + t_{ij}^M\right)$ is total stress tensor. t_{ij} and t_{ij}^M are magnetoelastic and Maxwell stress tensors, respectively, and they can be expressed by

$$t_{ij} = \sigma_{ij} + \frac{\mu_0}{\chi}M_i^0 M_k^0 + \frac{\mu_0}{\chi}(M_i^0 m_j + M_j^0 m_i), \tag{7}$$

$$t_{ij}^M = \mu_1 H_i^0 H_j^0 - \frac{1}{2}\mu_0 H_k^0 H_k^0 \delta_{ij} + \mu_1(H_i^0 h_j + H_j^0 h_i) - \mu_0 H_k^0 h_k \delta_{ij}. \tag{8}$$

In Eq. (7), σ_{ij} is the elastic stress tensor

$$\sigma_{ij} = \lambda\delta_{ij}u_{k,k} + G(u_{i,j} + u_{j,i}), \tag{9}$$

where δ_{ij} is Kronecker delta, and λ and G are Lame constants.

Substituting Eqs. (7) and (8) into (6) leads to

$$t_{ij,i} + \mu_0\left(M_i^0 H_{j,i}^0 + M_i^0 h_{j,i} + m_i H_{j,i}^0\right) = 0. \tag{10}$$

On the traction-free boundary, the boundary conditions are [4]:

$$e_{ijk}\{n_j[\![h_k]\!] - n_m u_{m,j}[\![H_k^0]\!]\} = 0, n_i[\![b_i]\!] - n_m u_{m,i}[\![B_i^0]\!] = 0, \tag{11}$$

$$n_i[\![t_{ij} + t_{ij}^M]\!] = 0. \tag{12}$$

Below we first solve the magneto-static problem for the rigid body state based on the boundary condition of Eq. (4), and then derive the solutions for the perturbation state using Eqs. (11) and (12).

3. Solution for rigid body state

Consider a 2D problem of a soft ferromagnetic solid with a single crack as shown in Fig. 1. We assume that the solid is only subjected to a uniform magnetic loading B_2^∞ at infinity. Thus, Eq. (2) becomes

$$H_{1,2}^0 - H_{2,1}^0 = 0, \tag{13a}$$

$$B_{1,1}^0 + B_{2,2}^0 = 0. \tag{13b}$$

If we let

$$H_1^0 = \frac{\partial\varphi_0}{\partial x}, \quad H_2^0 = \frac{\partial\varphi_0}{\partial y}. \tag{14}$$

Then Eq. (13a) is automatically satisfied, and Eqs. (3), (13b) and (14) lead to

$$\nabla^2\varphi_0 = 0, \tag{15}$$

where $\nabla^2 = \frac{\partial^2}{\partial x^2} + \frac{\partial^2}{\partial y^2}$.

We define

$$\varphi_0(x_1, x_2) = Re[W_0(z)], \quad z = x_1 + ix_2,$$

where $W_0(z)$ is an analytical complex potential function, by using Eqs. (14) and (3). It can be obtained that

$$H_1^0 - iH_2^0 = W_0'(z), \tag{16a}$$

$$B_1^0 - iB_2^0 = \mu_1 W_0'(z). \tag{16b}$$

Hence, for this case, Eq. (4) gives

$$B_2^0 = B_2^{0(e)}, \quad H_1^0 = H_1^{0(e)}, \tag{17}$$

where the quantities with the superscripts "(e)" represent those inside the crack.

Neglecting the change of magnetic fields within the crack along the x_2-direction, Eq. (17) is reduced to

$$B_2^{0+}(x_1) = B_2^{0-}(x_1), \quad H_1^{0+}(x_1) = H_1^{0-}(x_1) \tag{18}$$

which show that the crack behaves as a magnetically permeable slit.

Now, from Eqs. (16) and (18), and using the single-valued condition of magnetic potential, we finally obtain

$$W_0'(z) = -\frac{i}{\mu_1}B_2^\infty. \tag{19}$$

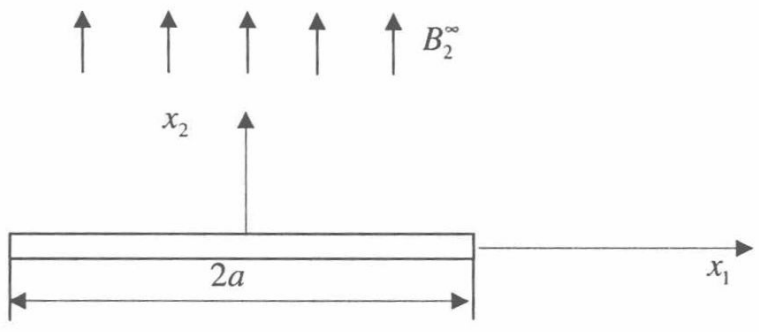

Fig. 1. A crack in a soft ferromagnetic solid.

Eqs. (19) and (16) show that in the rigid body state, the magnetic fields in the medium are *uniform*. That is,

$$B_1^0 = 0, \quad H_1^0 = 0, \quad B_2^0 = B_2^\infty, \quad H_2^0 = \frac{B_2^\infty}{\mu_1}, \quad M_1^0 = 0, \quad M_2^0 = \chi \frac{B_2^\infty}{\mu_1}. \tag{20}$$

Inside the crack, however, the components of uniform magnetic fields are

$$B_1^{0(e)} = 0, \quad H_1^{0(e)} = 0, \quad M_1^{0(e)} = 0, \quad M_2^{0(e)} = 0, \quad B_2^{0(e)} = B_2^\infty, \quad H_2^{0(e)} = \frac{B_2^\infty}{\mu_0} = \frac{\mu_1}{\mu_0} H_2^0. \tag{21}$$

Indeed, for an infinite soft ferromagnetic solid with arbitrary cracks, it can be shown that the magnetic field in the solid is always uniform and equal to the applied one at infinity. That is, the crack has no effect on the disturbance of magnetic fields in the rigid body state.

4. Field expressions for perturbation state

For the perturbation state, field equations are also given in the form of complex potentials by Fil'shtinkskii [15]. However, these equations were presented only for the magnetoelastic stresses t_{ij}. For comparison with purely elastic cases, here we derive the field expressions for the elastic stress tensor σ_{ij}.

To do this, we have from Eq. (5):

$$h_{1,2} - h_{2,1} = 0, \tag{22a}$$

$$b_{1,1} + b_{2,2} = 0. \tag{22b}$$

If we let

$$h_1 = \frac{\partial \zeta}{\partial x}, \quad h_2 = \frac{\partial \zeta}{\partial y}. \tag{23}$$

Eq. (22a) is automatically satisfied, and Eq. (22b) yields

$$\nabla^2 \zeta = 0. \tag{24}$$

Similarly, we have

$$\zeta = Re[w(z)], \tag{25a}$$

$$h_1 - ih_2 = w'(z), \tag{25b}$$

$$b_1 - ib_2 = \mu_1 w'(z), \tag{25c}$$

where $w(z)$ is an analytical complex potential function. However, from Eq. (10), we have

$$t_{11,1} + t_{21,2} + \frac{\chi B_2^\infty}{\mu_r} h_{1,2} = 0, \tag{26a}$$

$$t_{12,1} + t_{22,2} + \frac{\chi B_2^\infty}{\mu_r} h_{2,2} = 0, \tag{26b}$$

where t_{ij} is given by Eq. (7) in combination with Eqs. (20) and (21). Thus,

$$t_{11} = \sigma_{11},$$

$$t_{22} = \sigma_{22} + \frac{\chi (B_2^\infty)^2}{\mu_0 \mu_r^2} + \frac{2\chi B_2^\infty h_2}{\mu_r},$$

$$t_{12} = t_{21} = \sigma_{12} + \frac{\chi B_2^\infty h_1}{\mu_r}. \tag{27}$$

By substituting Eq. (27) into Eq. (26), and noting from Eqs. (23) and (24), $h_{1,2} = h_{2,1}$ and $h_{1,1} + h_{2,2} = 0$, we obtain

$$\sigma_{11,1} + \sigma_{12,2} + 2\frac{\chi B_2^\infty}{\mu_r} h_{2,1} = 0, \tag{28a}$$

$$\sigma_{12,1} + \sigma_{22,2} + 2\frac{\chi B_2^\infty}{\mu_r} h_{2,2} = 0. \tag{28b}$$

Eq. (28) can be rewritten as [11]:

$$\sigma_{11,1} + \sigma_{12,2} + (-V_{,1}) = 0, \tag{29a}$$

$$\sigma_{12,1} + \sigma_{22,2} + (-V_{,2}) = 0, \tag{29b}$$

where

$$V = -2\frac{\chi B_2^{\infty}}{\mu_r} h_2 = -2\frac{\chi B_2^{\infty}}{\mu_r}\zeta_{,2}. \tag{30}$$

Now let

$$\sigma_{11} = \frac{\partial^2 U}{\partial x_2^2} + V, \quad \sigma_{12} = -\frac{\partial^2 U}{\partial x_1 \partial x_2}, \quad \sigma_{22} = \frac{\partial^2 U}{\partial x_1^2} + V, \tag{31}$$

where U denotes a real stress function. Then, Eq. (29) is automatically satisfied.

In addition, for the plane stress problem, the displacement compatibility condition requires

$$\nabla^2(\sigma_{11} + \sigma_{22}) = -(1+\mu)\nabla^2(-V), \tag{32}$$

where μ is the Poisson ratio. (For plane strain, the corresponding solutions can be obtained from the present plane stress case by replacing μ and E with $\mu/(1-\mu)$ and $E/(1-\mu^2)$, respectively.) With Eqs. (30) and (24), we have

$$\nabla^2(-V) = 2\frac{\chi B_2^{\infty}}{\mu_r}(\nabla^2\zeta)_{,2} = 0. \tag{33}$$

Thus, Eq. (32) becomes

$$\nabla^2(\sigma_{11} + \sigma_{22}) = 0. \tag{34}$$

Inserting Eq. (31) into (34) and then using Eq. (33), we have

$$\nabla^4 U = 0. \tag{35}$$

The general solution of Eq. (35) is [18]:

$$U = 2Re[\bar{z}\varphi(z) + \psi(z)], \tag{36}$$

where $\phi(z)$ and $\psi(z)$ are two complex functions. From Eq. (25b) we obtain

$$h_2 = -\frac{1}{2i}[w'(z) - \overline{w'(z)}]. \tag{37a}$$

$$h_1 = \frac{1}{2}[w'(z) + \overline{w'(z)}]. \tag{37b}$$

Putting Eq. (37a) into (30) gives

$$V = \frac{\chi B_2^{\infty}}{i\mu_r}[w'(z) - \overline{w'(z)}] = 2Re[c_3 w'(z)], \tag{38}$$

where

$$c_3 = \frac{\chi B_2^{\infty}}{i\mu_r}.$$

From Eqs. (31), (36) and (38), we finally obtain

$$\sigma_{22} + \sigma_{11} = 4Re[\varphi'(z) + c_3 w'(z)], \tag{39a}$$

$$\sigma_{22} - \sigma_{11} + 2i\sigma_{12} = 2[\bar{z}\varphi''(z) + \psi'^{(z)}]. \tag{39b}$$

Similarly, the displacements are given by (see Appendix A)

$$2G(u_1 + iu_2) = \kappa\varphi(z) - z\overline{\varphi'(z)} - \psi(z) + \hat{\kappa}c_3 w(z), \tag{40}$$

where $\kappa = (3-\mu)/(1+\mu), \hat{\kappa} = 2(1-\mu)/(1+\mu)$, $G = E/2(1+\mu)$ and E is Young's modulus.

From Eq. (39b) we have

$$\sigma_{22} - \sigma_{11} - 2i\sigma_{12} = 2[z\overline{\varphi''(z)} + \overline{\psi'(z)}]. \tag{41}$$

Thus, Eqs. (41) and (39b) give

$$\sigma_{22} - i\sigma_{12} = \varphi'(z) + \overline{\varphi'(z)} + z\overline{\varphi''(z)} + \overline{\psi'(z)} + c_3 w'(z) + \overline{c_3 w'(z)}. \tag{42}$$

Define a new function $\Omega(z)$ such that

$$\Omega(z) = \bar{\varphi}'(z) + z\bar{\varphi}''(z) + \bar{\psi}'(z) + \overline{c_3}\bar{w}'(z). \tag{43}$$